Engineering Science and Technology, an International Journal 60 (2024) 101892

Contents lists available at ScienceDirect

Engineering Science and Technology, an International Journal

journal homepage: www.elsevier.com/locate/jestch

Etching-free fabrication method for silver nanowires-based SERS sensors for enhanced molecule detection

Yurim Han [a,1], Cristiano D'Andrea [b,1], Mirine Leem [c], Ji-Won Jung [d], Sooman Lim [e,*], Paolo Matteini [b,*], Byungil Hwang [a,*]

[a] School of Integrative Engineering, Chung-Ang University, Seoul 06974, Republic of Korea
[b] Institute of Applied Physics "Nello Carrara", National Research Council, Via Madonna del Piano 10, 50019 Sesto Fiorentino, Italy
[c] School of Advanced Materials Science and Engineering, Sungkyunkwan University, Suwon 16419, Republic of Korea
[d] Department of Materials Science and Engineering, Konkuk University, Seoul 05029, Republic of Korea
[e] Graduate School of Flexible and Printable Electronics, LANL-JBNU Engineering Institute-Korea, Jeonbuk National University, Jeonju 54896, Republic of Korea

ARTICLE INFO

Keywords:
Surface-enhanced Raman spectroscopy
Silver nanowires
Dry film photoresist
Lift-off process
Sensor

ABSTRACT

Surface-enhanced Raman spectroscopy (SERS) has garnered increasing attention for its ability to detect molecules even at low concentrations; however, the fabrication methods for SERS sensors require further study aimed at simple and rapid on-body and environmental monitoring. In this context, we propose an etching-free method for fabricating silver nanowires (AgNWs)-SERS sensors based on AgNWs. A lift-off process was conducted to create a pattern without etching, and lamination of the dry film resist overcame the limitations associated with liquid photoresists. Consequently, the resulting AgNW-patterned substrate was used to evaluate the pH of the test solution in the range of 1.1 and 12.0 and exhibited a Raman signal enhancement of 2×10^6. This fast and cost-effective fabrication method, combined with the intrinsic flexibility of the substrate and rapid and reproducible response to pH variations, provides a foundation for applying AgNW-patterned substrates for microenvironmental analysis or developing wearable optical devices.

1. Introduction

With increasing demand for personal medical diagnostics, various sensing techniques for disease and microenvironmental monitoring have been actively investigated. Among these techniques, surface-enhanced Raman spectroscopy (SERS), which can be employed to develop optical analysis sensors and portable biodetection devices, is considered the most promising [1–4]. Raman spectroscopy is a rapid, non-invasive, and non-destructive method for characterizing the structural and chemical nature of molecules using inelastically scattered light [5–7]. However, it has limitations owing to its relatively weak signal [8,9]; thus, enhancing Raman emission is essential for practical sensing applications. Consequently, SERS has been proposed as an effective method for enhancing Raman signals [51,10–12].

Compared to Raman spectroscopy, SERS provides the same chemo-structural information but enables considerable signal enhancement owing to the optical properties of noble metal nanoparticles (NPs). When exposed to light, free electrons on the surface of metal nanoparticles oscillate, producing a local surface plasmon (LSP) effect. When the incident light frequency corresponds to the oscillation frequency of the LSP, the resonance effect is termed as localized surface plasmon resonances (LSPRs) [13]. Owing to LSPR, a localized enhancement of the electromagnetic field is observed in the regions (hotspots) in close proximity to metal nanoparticles or in the gap between them [9,14,15]. This amplifies the scattered light emission and enables an increased signal strength, making SERS suitable for characterizing molecules at sub-micromolar concentrations or for sensor applications [16,17]. Silver, gold, and copper are representative SERS materials because of their LSPR at visible light wavelengths, which supports the usability of SERS sensors [18,19]. Although various nanostructures have been explored due to the strong LSPR observed in rod-like morphologies or sharp edges, silver nanowires (AgNWs), with their high aspect ratio, offer

Abbreviations: **SERS**, surface-enhanced Raman spectroscopy; **AgNW**, silver nanowire; **LSPR**, localized surface plasmon resonance; NP, nanoparticle; **PR**, photoresist; **DFR**, dry film resist; **PTFE**, polyetrafluoroethylene; **FCG**, film-combined glass; **4-MBA**, 4-mercaptobenzoic acid.

* Corresponding authors.
E-mail addresses: smlim@jbnu.ac.kr (S. Lim), p.matteini@ifac.cnr.it (P. Matteini), bihwang@cau.ac.kr (B. Hwang).

[1] These authors contributed equally to this work.

https://doi.org/10.1016/j.jestch.2024.101892
Received 23 July 2024; Received in revised form 2 October 2024; Accepted 1 November 2024
Available online 16 November 2024
2215-0986/© 2024 The Author(s). Published by Elsevier B.V. on behalf of Karabuk University. This is an open access article under the CC BY-NC-ND license (http://creativecommons.org/licenses/by-nc-nd/4.0/).

notable advantages for signal enhancement [20]. Antenna-like electromagnetic resonances that occur in AgNWs strongly enhance the Raman scattering of the molecules [21]. Additionally, the tunability of their size/length, scalability, and affordability when compared to gold nanowires make AgNWs ideal candidates for SERS detection [22–24]. In addition to the detection of low-concentration analytes in sweat via signal enhancement from Raman scattering, it also has advantages for pH monitoring, such as real-time response and noninvasiveness, when compared to traditional time-consuming methods [25].

For practical applications in real-time SERS detection, SERS substrates have attracted significant attention to overcome the problems of SERS dispersion due to random distribution and potential aggregation in terms of the reproducibility and reliability of SERS analysis [5,8,26,27]. This in turn also limits the portability and on-site use of sensors. Therefore, the fabrication of metal nanostructures on substrates for use in next-generation sensors has been extensively examined [28]. Yang et al. [29] prepared a SERS substrate by spraying silver nanoparticles and gold nanoparticles (AgNPs and AuNPs, respectively) through a designed panel with uniform dimensions. Banchelli et al. [16] deposited AgNWs on Teflon using flow-through filtration and laser patterning. Ricci et al. [19] coated AuNP ink onto glass substrates, and Kumar et al. [20] fabricated an AgNP dot array on a polyethylene naphthalate film via inkjet printing [30,31]. Photolithography using a liquid photoresist (PR) is one of the various methods, including spin coating, thermal baking, UV exposure, development, etching, and stripping. However, photolithography using liquid PR has limitations in terms of the fabrication process and application. First, achieving a uniform layer thickness and pattern size using liquid PR is challenging, with additional time and costs incurred to evaporate the solvent after spin coating [32,33]. Additionally, photolithography employs toxic etchants that can damage the nanoparticle network and render the SERS substrate unsuitable for wearable sensors, thereby affecting its safety for human use [34,35]. In terms of applications, while appropriate for smooth and rigid substrates, liquid PR is not suitable for robust or flexible polymeric substrates [36]. Furthermore, the heat treatment required for the thermal baking of liquid PR can damage the substrate, limiting the types of substrates that can be used and restricting their application under deformable conditions [47–49].

Hence, the use of a dry film resist (DFR) has been recommended as an alternative to liquid PR, with the employment of a lift-off process, in gaining traction to create patterns without the need for etching. DFR is a solid-state thin film that allows lamination of a uniform layer and simplifies the patterning process, thus making it faster, more cost-effective, and suitable for large-scale production, including roll-to-roll processes [37]. Furthermore, DFR results in the absence of edge beads, leading to nearly vertical sidewalls [38]. Additionally, the lift-off process is effective for pattern creation for SERS sensors without requiring etching, which can harm the substrate and reduce the biocompatibility of the sensor, particularly in the case of wet etching [39]. Conventional lift-off processes involve PR coating, UV exposure, development, coating, and stripping. A PR is typically spin-coated onto a substrate, and after UV exposure, the UV-exposed PR is selectively removed during development. Finally, the remaining PR layer serves as a template for the desired pattern during the coating of patterned materials, followed by stripping [40]. The lift-off process excludes etchant residues, making it suitable for flexible devices and offering compatibility for easy integration with other fabrication processes [39].

In this study, we propose an etching-free fabrication method for an AgNW-based SERS sensor using a DFR via a lift-off process. DFR overcomes the limitations associated with liquid PR, offering simplicity, speed, and cost-effectiveness and ultimately enabling large-scale production. Moreover, the lift-off process allows the incorporation of flexible substrates into SERS sensors, making them suitable for deformable conditions and curved surfaces without etching. The SERS activity of the AgNW pattern, tested using a pH-sensitive molecule as a probe, demonstrated considerable SERS enhancement and the capability to monitor the pH of small aliquots of solution. We expect that the fabricated AgNW-patterned substrate can be used as a SERS sensor for the effective detection of marker molecules in various environments, as well as in the development of SERS wearable devices for biofluid analysis or as a SERS-active tool for optical pH monitoring.

2. Materials and methods

2.1. Materials and experiment

In this study, we employed a polyetrafluoroethylene (PTFE) membrane filter (pore size: 0.45 μm, Hyundai Micro, PTFE2025D), DFR with a thickness of 15 μm (KOLON Industries, KL-1015), and an AgNW dispersion (diameter: 60 nm; length: 3 μm; 1 wt%; dispersed in isopropyl alcohol; capped with PVP, Flexio). TEM image of AgNW is shown in Figure S1. The AgNW-patterned substrate was fabricated using a DFR via a lift-off process. Initially, the DFR was laminated onto a PTFE membrane filter using a laminator (Jaesung Engineering, JSL-1200). Subsequently, UV exposure was performed under vacuum using a film-combined glass (FCG) mask with a specified pattern size of 2 mm. For the development and stripping processes, solutions of Na_2CO_3 (Samchun Chem) and NaOH (Samchun Chem) were prepared at concentrations of 1 and 4 wt%, respectively. AgNW patterns were created via vacuum filtration. AgNW-patterned substrates were maintained under vacuum conditions until use, and a recent study by our group [41] demonstrated their stable SERS response.

2.2. Characterization and measurement methods

The fabricated AgNW patterns were characterized using scanning electron microscopy (SEM; SIGMA 300). Its morphology was analyzed via atomic force microscopy (AFM) in the tapping mode using a JPK Nanowizard III Sense scanning probe microscope (Bruker) equipped with a single-beam silicon cantilever (μMash, HQ:NSC15 Cr-Au BS). The drive frequency was set between 250 and 300 kHz, and the scan rate was set to 0.5 Hz. The optical transmittance was measured using a haze meter (Haze Guard I, BYK instrument, Germany). The sheet resistance was measured using a four-point probe system (Robo-I, YoungIn Co. Ltd., Korea).

SERS analysis was conducted using a Horiba LabRam HR800 evolution micro-Raman spectrometer coupled with a 785-nm laser excitation source. The laser beam (waist dimension: 2 μm; focal depth: 1.1 μm) was focused onto the sample via a 50× long working distance (LWD) objective (Olympus, NA 0.50). Raman-scattered light was collected by the same objective in the backscattering geometry, analyzed using a 600 grooves/mm grating, and finally acquired using a Peltier-cooled CCD detector (Syncerity, Horiba). Laser power onto the sample and spectra acquisition time were fixed at 100 μW and 5 s, respectively. The SERS spectra were analyzed and processed using LabSpec 6 (Horiba) and OriginPro (OriginLab) software.

As a Raman probe, a 4-mercaptobenzoic acid (4-MBA) solution was obtained by dissolving the purchased powder (Merck) in ethanol at a concentration of 5 mM. For the SERS experiments, the AgNW pattern was incubated overnight in 4-MBA solution, washed in ethanol, and dried in air. The maximum relative standard deviation (RSD) in the SERS signal (peak of approximately 1592 cm^{-1}), which did not exceed 10 %, was observed among the different substrate replicates.

Moreover, a human sweat model solution was prepared to test the capability of the AgNW-patterned substrate to evaluate the pH levels of a complex fluid, mimicking a real bio-sample such as sweat secretions. Specifically, a simulated sweat (SS) solution was created by mixing 0.1 % (w/v) urea, 0.1 % (w/v) lactate, and 0.5 % (w/v) NaCl in ultrapure water (chemicals purchased from Merck) and adjusting the pH to three different values (4.9, 6.6, and 9.0) using phosphate buffer. These pH values were selected to reflect the average physiological pH of human sweat and potential fluctuations due to pathological conditions.

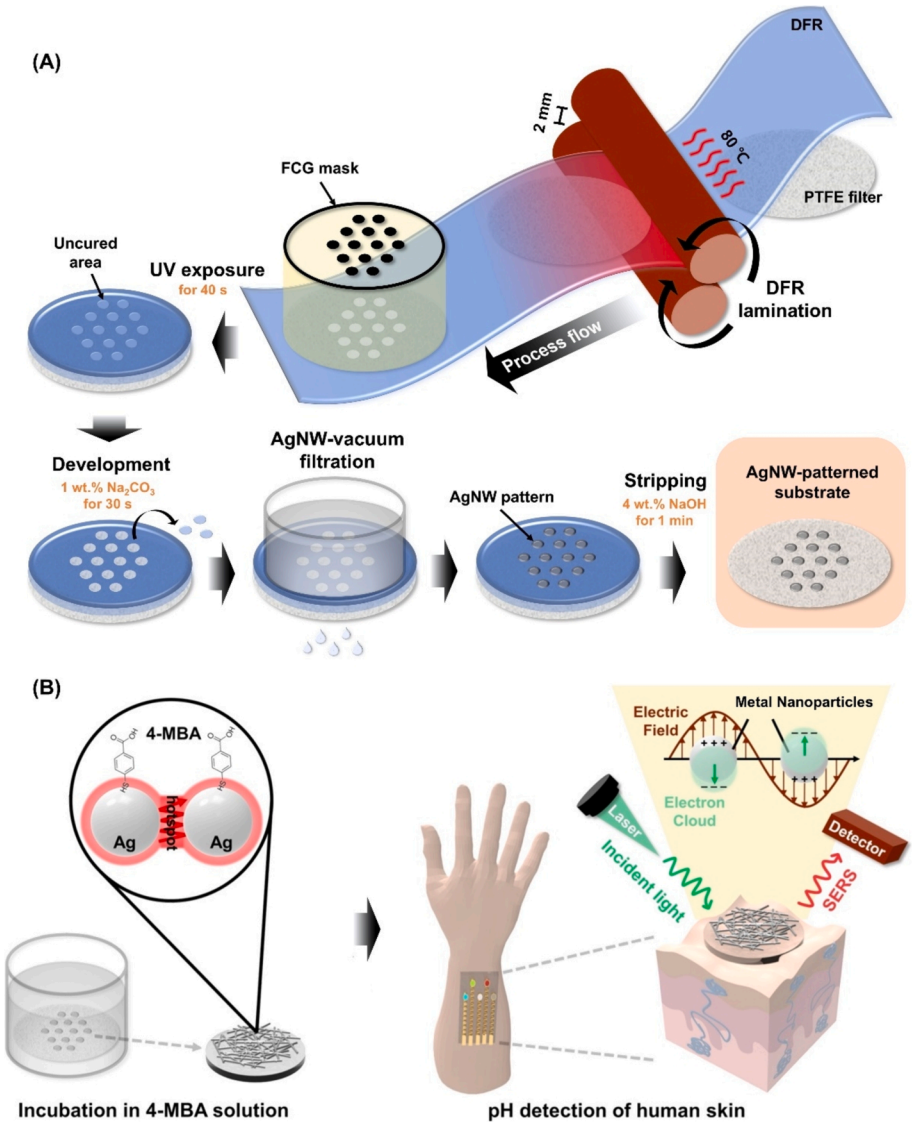


Fig. 1. (A) Schematic of patterning AgNW on PTFE membrane filter using DFR via lift-off process and (B) illustration of procedure for detecting SERS signal on human skin.

3. Results and discussion

3.1. Fabrication of AgNW-patterned substrate

Fig. 1 illustrates a schematic of the lift-off process using the DFR. To facilitate handling, the PTFE membrane filter was supported by a polypropylene layer with an AgNW pattern on the PTFE side. The process began with coating the PTFE membrane filter with DFR through lamination in a roll gap of 2 mm at 80 °C. The DFR-coated PTFE membrane filter was then exposed to UV light for 40 s via an FCG mask, and the exposed area was cured due to using a negative-type DFR. A circular-pattern mask was selected for this process because it is advantageous for drop deposition detection [16,32].

Following the UV exposure, a non-cured area was developed by immersing it in a 1 wt% Na_2CO_3 solution for 30 s. This step removes the uncured DFR following the following chemical reaction [42], leaving behind a cured DFR that acts as a template for the desired pattern.

$$Na_2CO_3^- \leftrightarrow Na^+ + NaCO_3^-$$

$$Na_2CO_3^- + H_2O \leftrightarrow NaHCO_3 + OH^-$$

$$DFR - COOH + Na^+ + OH^- \rightarrow DFR - COONa^+ + H_2O$$

The AgNW dispersion was vacuum filtered through the developed area for 1 min to fabricate the AgNW patterns. Subsequently, the filtered PTFE membrane was immersed in 4 wt% NaOH solution for 1 min to eliminate any remaining cured DFR, leaving only the AgNW patterns on the substrate, according to the following reaction [43]:

$$NaOH \leftrightarrow Na^+ + OH^-$$

$$DFR - COOH + OH^- \rightarrow DFR - COONa^+ + H_2O$$

3.2. Surface characterization

The resulting patterns were characterized using SEM and AFM. Fig. 2 clearly shows the successful fabrication of a circular pattern on the PTFE membrane filter, confirming pattern uniformity on the millimeter scale. The morphology of the AgNW patterns was further investigated using tapping-mode AFM [50]. Fig. 2D shows a 3 × 3 μm^2 scan of the AgNWs layer. A randomly distributed network of NWs is visible: single NW with an average diameter of 60 nm and a length of a few microns are intertwined or crossed with each other, forming several SERS active hotspots,

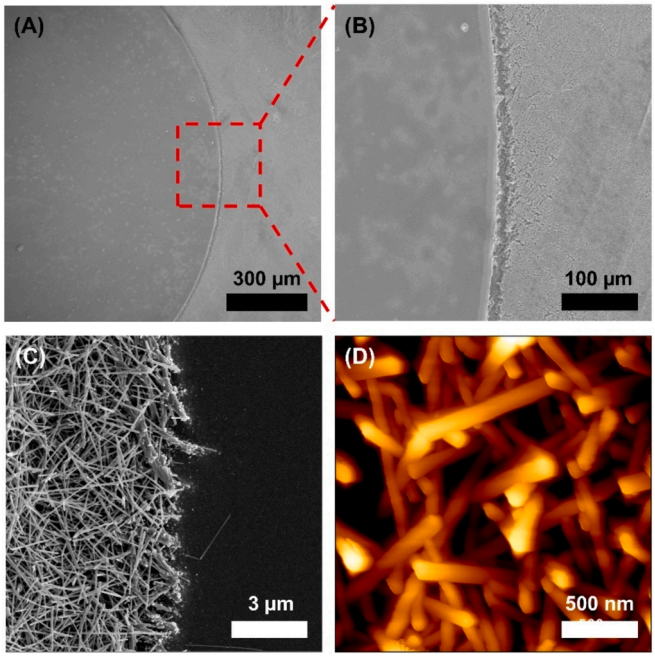


Fig. 2. (A–C) SEM images under various magnifications. (D) Tapping-mode AFM image of AgNW-patterned substrate.

as demonstrated by the theoretical simulation of the E-field distribution, as recently shown by our group [16]. Additionally, the advantages of patterned AgNWs for SERS detection over the entire layer were demonstrated in our previous study [16]. An identical micrometric volume of the analyte was deposited on a single AgNW spot and on an entire plain silver NWs layer. The SERS maps acquired from both supports demonstrated a two-fold signal intensity increase, with a more homogeneous distribution and minimal signal fluctuation (relative standard deviation of less than 10 %) from the spotted sample, owing to the maximized interaction between the analyte molecule and SERS-active silver surface.

To confirm that no AgNWs were lost during the DFR process, we prepared non-patterned AgNW networks that underwent full DFR lamination, baking, development, and stripping. We measured the optical transmittance and sheet resistance of bare AgNW networks and those subjected to DFR patterning. The bare AgNW networks exhibited an optical transmittance of approximately 82.3 % at a wavelength of 550 nm and a sheet resistance of approximately 92.2 Ω/cm. After DFR, AgNW networks exhibited similar values, with an optical transmittance of approximately 82.1 % and a sheet resistance of approximately 91.9 Ω/cm. These consistent optical and electrical properties before and after the DFR process indicate that no significant loss of AgNWs occurred during patterning. The sharp patterning of AgNWs, confirmed by SEM and AFM images, without any significant degradation in the electrical or optical performance further supports the effectiveness of the DFR patterning process for preparing SERS substrates.

3.3. Evaluation of SERS sensing

To evaluate its applicability for SERS sensing, the fabricated AgNW-patterned substrate was soaked with 4-MBA molecules. A Raman probe, which typically forms covalent and stable bonds with noble metal nanoparticles through thiol groups, characterized by intense Raman activity mainly correlated to benzene ring breathing. Fig. 3A shows a comparison between the SERS spectra of the AgNW pattern before (blue line) and after (red line) 4-MBA incubation, whereas the right panel (Fig. 3B) shows the Raman spectra of a 5-mM ethanolic solution of 4-MBA (brown line) and ethanol (green line).

The SERS spectra of 4-MBA clearly exhibited intense vibrations due to CC ring stretching at 1080 and 1592 cm^{-1}, whereas the doublet modes related to CH stretching (1140 and 1185 cm^{-1}) and bending vibration modes assigned to CO and CH peaks at 845 and 1485 cm^{-1}, respectively, exhibited less intense but still clearly detectable vibrations. Furthermore, the SERS spectra showed a band at 1400–1425 cm^{-1}, related to $COOH/COO^-$ Raman vibrations that notably shifted in intensity and frequency in response to different pH values [44].

The SERS enhancement factor (EF) of AgNW-patterned substrate was estimated by comparing the intensity (I_{SERS}) of the mode centered at 1592 cm^{-1} observed in the SERS spectra of 4-MBA (Fig. 3A) and intensity (I_{Raman}) of the corresponding mode detectable in Raman spectra of 4-MBA in ethanolic solution (Fig. 3B). The EF was calculated according to equation $(I_{SERS}/I_{Raman}) \times (N_{Raman}/N_{SERS})$, where N_{Raman} and N_{SERS} are the number of molecules responsible for the Raman and SERS signals, respectively. Furthermore, Raman and SERS intensities were normalized by the laser power applied to the sample and integration times of the acquired spectra. More specifically, N_{SERS} was calculated as the number of 4-MBA molecules, forming a monolayer on the SERS-active hotspots on the AgNW-patterned layer according to equation $N_{SERS} = D_{AgNWs} \times A_{waist} \times A_{eff}/f_p$), where D_{AgNWs} denotes the AgNW density on PTFE, A_{eff} denotes the effective area of the hotspot, and f_p denotes the footprint area of the 4-MBA molecules [16]. Furthermore, N_{Raman} denotes the number of molecules contained in the focal volume of the laser spot according to the following formula:

$$N_{Raman} = C_{4-MBA} \times V_f \times NA = C_{4-MBA} \times A_{waist} \times H_{depth} \times NA$$

where $C_{4\text{-}MBA}$ denotes the concentration of 4-MBA molecules in the ethanol solution used for the Raman experiments, V_f denotes the focal

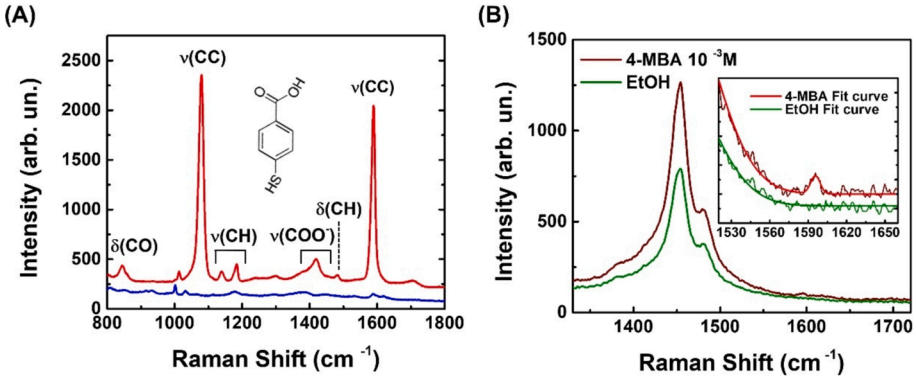


Fig. 3. (A) SERS spectra of AgNW-patterned substrate before (blue line) and after (red line) incubation with 4-MBA solution. Main Raman modes related to 4-MBA vibrations are assigned (*∂*: deformation; *ν*: stretching). (B) Raman spectrum of a 5-mM ethanolic solution of 4-MBA. The inset highlights the peak at 1594 cm^{-1}, attributed to CC ring stretching vibration of 4-MBA, which is absent in the Raman spectrum of ethanol (green line) and is used for the calculation of SERS EF.

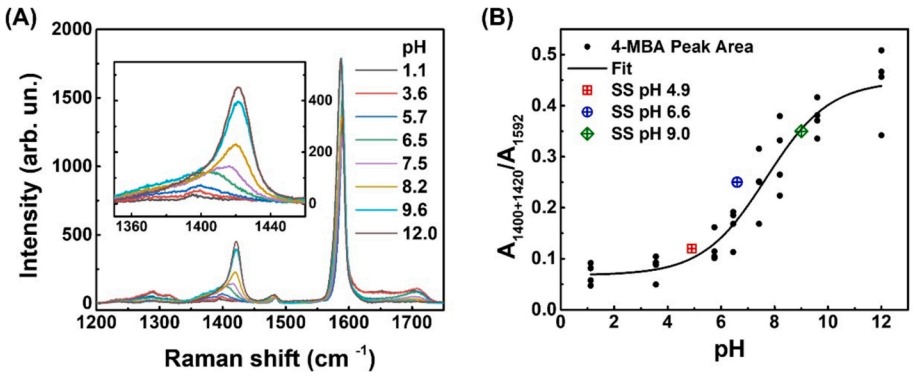


Fig. 4. (A) SERS spectra of AgNW-patterned substrate after functionalization with 4-MBA and incubation with a PBS buffer solution at different pH values. The inset highlights the shift and intensity increase of the band in the 1400–1420 cm^{-1} region. (B) Calibration curve obtained considering the area of the band in the 1400–1420 cm^{-1} interval, related to the COOH group vibrations and normalized for the area of the benzene ring breathing peak centered at 1592 cm^{-1}. The AgNWs-patterned substrate was tested with three SS solutions at different pH values, and the obtained results were denoted by red, blue and green geometrical symbols.

volume, A_{waist} denotes the laser spot area in the focal plane, H_{depth} denotes the depth of field of the 50× LWD objective, and NA denotes Avogadro's number.

Considering $D_{AgNWs} = 1.6 \times 10^6$ AgNWs/mm^2, $A_{eff} = 5 \times 10^4$ nm^2, $f_p = 0.44$ nm^2/mol for 4-MBA as well as $H_{depth} = 1.1$ μm, we calculated a value of 1.8×10^4 for N_{Raman}/N_{SERS}. Based on this, with I_{SERS}/I_{Raman} of approximately 120 ($I_{SERS} = 1700$ counts and $I_{Raman} = 14$ counts), an EF value of 2×10^6 was estimated [45].

The intrinsic pH-sensing capability of the 4-MBA molecules, deposited on the AgNW patterned layer, was exploited. A set of SERS experiments are performed by depositing a 2-μL drop of a 1x PBS buffer solution with a wide range of pH values between 1.1 and 12.0 on single AgNW spots, as introduced in Fig. 2. The pH values were obtained by adding 0.1 M HCl or NaOH (Fig. 4A). The observable shift and intensity increase in the band in the 1400–1420 cm^{-1} region denotes the progressive deprotonation of the COOH groups at increasing pH values [46]. Normalizing the area of the band at 1400–1420 cm^{-1} to the area of the benzene Raman mode at 1592 cm^{-1} resulted in the calibration curve shown in Fig. 4B, demonstrating the feasibility of using the AgNW pattern for the evaluation of pH within a wide pH range. The ability of the AgNW-patterned substrate to monitor pH was further tested using a SS solution at three fixed pH levels. The results are reported in Fig. 4B, where the normalized areas of the 1400–1420 cm^{-1} band are represented by geometrical symbols (a red square, blue circle, and green diamond), corresponding to pH values of 4.9, 6.6, and 9.0, respectively. In all cases, data were within the 95% prediction interval.

4. Conclusions

We successfully prepared AgNW-patterned substrates using an etching-free fabrication method and evaluated their applicability to SERS sensing. We employed the DFR replacing the liquid PR and laminated it onto a PTFE membrane filter without thermal baking, which could potentially damage the substrate. During the lift-off process, we obtained AgNW patterns without using typical toxic etchants; instead, we employed a mildly alkaline solution for the development and stripping processes. Both SEM images confirmed the fabrication of the circular AgNW pattern, whereas the AFM topography confirmed the formation of intertwined NW structures within the layer. SERS analysis demonstrated the capability of the AgNW-patterned substrate to enhance the Raman signals of the 4-MBA molecules, selected here as probes, by up to 2×10^6 orders of magnitude. Further SERS experiments, exploiting the Raman sensitivity following the structural variation of the 4-MBA molecules with pH, demonstrated the applicability of the 4-MBA functionalized AgNW pattern as a suitable substrate for optical pH sensing.

In conclusion, the AgNW-patterned substrate, owing to its flexibility, speed, cost-effectiveness, and industrial scalability of the production process, as well as its effective SERS activity and pH-sensing capability, provides the foundation for developing optical devices for micro-pH evaluation in various environments, thus allowing the sampling of a few microliters of solution and overcoming one of the limitations of standard pH meters that typically require milliliters of analyte. Additionally, the results demonstrate the potential of AgNW patterns for use in flexible sensors due to their compatibility with biocompatible tapes or microfluidic polydimethylsiloxane (PDMS) layers. The development of SERS-based wearable devices is expected to be actively pursued for the detection and analysis of biofluids in on-body applications [44].

CRediT authorship contribution statement

Yurim Han: Writing – original draft, Visualization, Investigation, Formal analysis, Data curation. **Cristiano D'Andrea:** Writing – original draft, Validation, Formal analysis, Data curation. **Mirine Leem:** Writing – original draft, Visualization, Data curation. **Ji-Won Jung:** Validation, Writing – review & editing. **Sooman Lim:** Writing – original draft, Investigation, Formal analysis. **Paolo Matteini:** Writing – review & editing, Writing – original draft, Investigation, Funding acquisition, Data curation. **Byungil Hwang:** Writing – original draft, Visualization, Supervision, Funding acquisition, Formal analysis, Data curation, Conceptualization.

Declaration of competing interest

The authors declare that they have no known competing financial interests or personal relationships that could have appeared to influence the work reported in this paper.

Ackowledgement

This research was supported by the National Research Foundation of Korea (NRF) and funded by the Ministry of Science and ICT (MSIT) (RS-2024-00413272). This study was developed within the project funded by Next Generation EU - "Age-IT - Ageing well in an ageing society" project (PE0000015), National Recovery and Resilience Plan (NRRP) - PE8 - Mission 4, C2, Intervention 1.3" and Next Generation EU - 'Ecosistema dell'Innovazione' project (ECS00000017), and National Recovery and Resilience Plan (NRRP) - Tuscany Health Ecosystem (THE), Spoke 4: Nanotechnologies for diagnosis and therapy. The views and opinions expressed are only those of the authors and do not necessarily reflect those of the European Union or the European Commission. Neither the European Union nor the European Commission are responsible for this. Paolo Matteini and Byungil Hwang acknowledge the financial support from the Ministry of Foreign Affairs and International

Cooperation of Italy (MAECI) and the National Research Foundation of Korea (NRF) through the DESWEAT project (no. _PGR01065; NRF-2019K1A3A1A25000230) funded within the framework of the Executive Program of Scientific and Technological Cooperation between the Italian Republic and Korean Republic 2019-2021. This work was supported by the National Research Foundation of Korea (NRF) grant funded by the Government of Korea (NRF-RS-2023–00336593).

Appendix A. Supplementary data

Supplementary data to this article can be found online at https://doi.org/10.1016/j.jestch.2024.101892.

References

[1] X. Liu, J. Ma, P. Jiang, J. Shen, R. Wang, Y. Wang, G. Tu, Large-scale flexible surface-enhanced Raman scattering (SERS) sensors with high stability and signal homogeneity, ACS Appl. Mater. Interfaces 12 (40) (2020) 45332–45341, https://doi.org/10.1021/acsami.0c13691.

[2] M. Sanchez-Purra, B. Roig-Solvas, C. Rodriguez-Quijada, B. Leonardo, K. Hamad-Schifferli, Reporter selection for nanotags in multiplexed surface enhanced raman spectroscopy assays, ACS Omega 3 (9) (2018) 10733–10742, https://doi.org/10.1021/acsomega.8b01499.

[3] S. Lin, X. Lin, S. Han, Y. Liu, W. Hasi, L. Wang, Flexible fabrication of a paper-fluidic SERS sensor coated with a monolayer of core-shell nanospheres for reliable quantitative SERS measurements, Anal. Chim. Acta 1108 (2020) 167–176, https://doi.org/10.1016/j.aca.2020.02.034.

[4] E. Karooby, H. Sahbafar, M.H. Heris, A. Hadi, V. Eskandari, Identification of low concentrations of flucytosine drug using a surface-enhanced Raman scattering (SERS)-active filter paper substrate, Plasmonics 19 (2) (2023) 855–863, https://doi.org/10.1007/s11468-023-02042-1.

[5] L. Li, W. Chin, Rapid fabrication of a flexible and transparent Ag nanocubes@PDMS film as a SERS substrate with high performance, ACS Appl. Mater. Interfaces 12 (33) (2020) 37538–37548, https://doi.org/10.1021/acsami.0c07178.

[6] P. Mosier-Boss, Review of SERS substrates for chemical sensing, Nanomaterials (Basel) 7 (6) (2017), https://doi.org/10.3390/nano7060142.

[7] P. Polykretis, M. Banchelli, C. D'Andrea, M. de Angelis, P. Matteini, Raman spectroscopy techniques for the investigation and diagnosis of Alzheimer's disease, Front. Biosci. (Schol Ed) 14 (3) (2022) 22, https://doi.org/10.31083/j.fbs1403022.

[8] S. Mahanty, S. Majumder, R. Paul, R. Boroujerdi, E. Valsami-Jones, C. Laforsch, A review on nanomaterial-based SERS substrates for sustainable agriculture, Sci. Total Environ. 950 (2024) 174252, https://doi.org/10.1016/j.scitotenv.2024.174252.

[9] H. Sahbafar, S. Mehmandoust, L. Zeinalizad, A. Mohsennezhad, M.H. Abbas, A. Hadi, V. Eskandari, Prepared plasmonic glass substrates via electrodeposition for detecting trace glucose: SERS, DFT, and FDTD investigations, Plasmonics 19 (4) (2023) 2087–2096, https://doi.org/10.1007/s11468-023-02126-y.

[10] J. Dieringer, A. McFarland, N. Shah, D. Stuart, A. Whitney, C. Yonzon, M. Young, X. Zhang, R. Van Duyne, Surface enhanced Raman spectroscopy: new materials, concepts, characterization tools, and applications, Faraday Discuss. 132 (2006) 9–26, https://doi.org/10.1039/b513431p.

[11] P. Stiles, J. Dieringer, N. Shah, R. Van Duyne, Surface-enhanced Raman spectroscopy, Annu. Rev. Anal. Chem. (Palo Alto, Calif) 1 (2008) 601–626, https://doi.org/10.1146/annurev.anchem.1.031207.112814.

[12] X. Lin, D. Lin, Y. Chen, J. Lin, S. Weng, J. Song, S. Feng, High throughput blood analysis based on deep learning algorithm and self-positioning super-hydrophobic SERS platform for non-invasive multi-disease screening, Adv. Funct. Mater. 31 (51) (2021), https://doi.org/10.1002/adfm.202103382.

[13] C. D'Andrea, A. Irrera, B. Fazio, A. Foti, E. Messina, O. Maragò, S. Kessentini, P. Artoni, C. David, P. Gucciardi, Red shifted spectral dependence of the SERS enhancement in a random array of gold nanoparticles covered with a silica shell: extinction versus scattering, J. Opt. 17 (11) (2015), https://doi.org/10.1088/2040-8978/17/11/114016.

[14] P. Matteini, M. Cottat, F. Tavanti, E. Panfilova, M. Scuderi, G. Nicotra, M. Menziani, N. Khlebtsov, M. de Angelis, R. Pini, Site-selective surface-enhanced Raman detection of proteins, ACS Nano 11 (1) (2017) 918–926, https://doi.org/10.1021/acsnano.6b07523.

[15] H. Wei, H. Xu, Hot spots in different metal nanostructures for plasmon-enhanced Raman spectroscopy, Nanoscale 5 (22) (2013) 10794–10805, https://doi.org/10.1039/c3nr02924g.

[16] M. Banchelli, C. Amicucci, E. Ruggiero, C. D'Andrea, M. Cottat, D. Ciofini, I. Osticioli, G. Ghini, S. Siano, R. Pini, M. de Angelis, P. Matteini, Spot-on SERS detection of biomolecules with laser-patterned dot arrays of assembled silver nanowires, ChemNanoMat 5 (8) (2019) 1036–1043, https://doi.org/10.1002/cnma.201900035.

[17] A. Barucci, C. D'Andrea, E. Farnesi, M. Banchelli, C. Amicucci, M. de Angelis, B. Hwang, P. Matteini, Label-free SERS detection of proteins based on machine learning classification of chemo-structural determinants, Analyst 146 (2) (2021) 674–682, https://doi.org/10.1039/d0an02137g.

[18] O. Volochanskyi, M. Švecová, V. Bartůněk, V. Prokopec, Electroless deposition via galvanic displacement as a simple way for the preparation of silver, gold, and copper SERS-active substrates, Colloids Surf. A Physicochem. Eng. Asp. 616 (2021), https://doi.org/10.1016/j.colsurfa.2021.126310.

[19] B. Sharma, R. Frontiera, A. Henry, E. Ringe, R. Van Duyne, SERS: Materials, applications, and the future, Mater. Today 15 (1–2) (2012) 16–25, https://doi.org/10.1016/s1369-7021(12)70017-2.

[20] M.K. Francis, B.K. Sahu, P.B. Bhargav, C. Balaji, N. Ahmed, A. Das, S. Dhara, Ag nanowires based SERS substrates with very high enhancement factor, Physica E: Low-Dimensional Syst. Nanostruct. 137 (2022), https://doi.org/10.1016/j.physe.2021.115080.

[21] M. Rycenga, C.M. Cobley, J. Zeng, W. Li, C.H. Moran, Q. Zhang, D. Qin, Y. Xia, Controlling the synthesis and assembly of silver nanostructures for plasmonic applications, Chem. Rev. 111 (6) (2011) 3669–3712, https://doi.org/10.1021/cr100275d.

[22] Y. Shi, L. He, Q. Deng, Q. Liu, L. Li, W. Wang, Z. Xin, R. Liu, Synthesis and applications of silver nanowires for transparent conductive films, Micromachines (Basel) 10 (5) (2019), https://doi.org/10.3390/mi10050330.

[23] L. Zhang, H. Li, G. Chu, L. Luo, J. Jin, B. Zhao, Y. Tian, Detection of 6-Mercaptopurine by silver nanowires-coated silicon wafer based on surface-enhanced Raman scattering spectroscopy, Colloids Surf. A Physicochem. Eng. Asp. 508 (2016) 309–315, https://doi.org/10.1016/j.colsurfa.2016.08.069.

[24] K.M. Kosuda, J.M. Bingham, K.L. Wustholz, R.P. Van Duyne, Nanostructures and Surface-Enhanced Raman Spectroscopy, 1, Academic Press, 2010.

[25] P.C. Guan, Q.J. Qi, Y.Q. Wang, J.S. Lin, Y.J. Zhang, J.F. Li, Development of a 3D hydrogel SERS chip for noninvasive, real-time pH and glucose monitoring in sweat, ACS Appl. Mater. Interfaces 16 (36) (2024) 48139–48146, https://doi.org/10.1021/acsami.4c10817.

[26] E. Kozhina, S. Bedin, N. Nechaeva, S. Podoynitsyn, V. Tarakanov, S. Andreev, Y. Grigoriev, A. Naumov, Ag-nanowire bundles with gap hot spots synthesized in track-etched membranes as effective SERS-substrates, Appl. Sci. 11 (4) (2021), https://doi.org/10.3390/app11041375.

[27] E. Yavuz, M. Sakir, M.S. Onses, S. Salem, E. Yilmaz, Advancements in reusable SERS substrates for trace analysis applications, Talanta 279 (2024) 126640, https://doi.org/10.1016/j.talanta.2024.126640.

[28] A. Chirumamilla, I. Moise, Z. Cai, F. Ding, K. Jensen, D. Wang, P. Kristensen, L. Jensen, P. Fojan, V. Popok, M. Chirumamilla, K. Pedersen, Lithography-free fabrication of scalable 3D nanopillars as ultrasensitive SERS substrates, Appl. Mater. Today 31 (2023), https://doi.org/10.1016/j.apmt.2023.101763.

[29] G. Yang, X. Fang, Q. Jia, H. Gu, Y. Li, C. Han, L. Qu, Fabrication of paper-based SERS substrates by spraying silver and gold nanoparticles for SERS determination of malachite green, methylene blue, and crystal violet in fish, Mikrochim. Acta 187 (5) (2020) 310, https://doi.org/10.1007/s00604-020-04262-2.

[30] S. Ricci, M. Buonomo, S. Casalini, S. Bonacchi, M. Meneghetti, L. Litti, High performance multi-purpose nanostructured thin films by inkjet printing: Au micro-electrodes and SERS substrates, Nanoscale Adv. 5 (7) (2023) 1970–1977, https://doi.org/10.1039/d2na00917j.

[31] S. Kumar, K. Namura, D. Kumaki, S. Tokito, M. Suzuki, Highly reproducible, large scale inkjet-printed Ag nanoparticles-ink SERS substrate, Results Mater. 8 (2020), https://doi.org/10.1016/j.rinma.2020.100139.

[32] C. Amicucci, H. Ha, P. Matteini, B. Hwang, Facile fabrication of silver-nanowire-based chips using dry-film photoresist for wearable optical detection, Fashion Text. 9 (1) (2022), https://doi.org/10.1186/s40691-022-00297-6.

[33] J. Schober, J. Berger, C. Eulenkamp, K. Nicolaus, G. Feiertag, Thick film photoresist process for copper pillar bumps on surface acoustic wave-wafer level packages, in: 2020 IEEE 8th Electronics System-Integration Technology Conference (ESTC), 2020, pp. 1–7, https://doi.org/10.1109/ESTC48849.2020.9229720.

[34] Y. Kim, N. Kwon, S. Park, C. Kim, H. Chau, M. Hoang, M. Cho, D. Choi, Patterned sandwich-type silver nanowire-based flexible electrode by photolithography, ACS Appl. Mater. Interfaces 13 (51) (2021) 61463–61472, https://doi.org/10.1021/acsami.1c19164.

[35] M. Xin, J. Li, Z. Ma, L. Pan, Y. Shi, MXenes and their applications in wearable sensors, Front. Chem. 8 (2020) 297, https://doi.org/10.3389/fchem.2020.00297.

[36] B. Hwang, P. Matteini, Review on dry film photoresist-based patterning of Ag nanowire flexible electrodes for wearable electronics, Fashion Text. 9 (1) (2022), https://doi.org/10.1186/s40691-022-00303-x.

[37] H. Kim, G. Lee, S. Becker, J. Kim, H. Kim, B. Hwang, Novel patterning of flexible and transparent Ag nanowire electrodes using oxygen plasma treatment, J. Mater. Chem. C 6 (35) (2018) 9394–9398, https://doi.org/10.1039/c8tc02377h.

[38] P. Mukherjee, F. Nebuloni, H. Gao, J. Zhou, I. Papautsky, Rapid prototyping of soft lithography masters for microfluidic devices using dry film photoresist in a non-cleanroom setting, Micromachines (Basel) 10 (3) (2019), https://doi.org/10.3390/mi10030192.

[39] L. Guo, S. DeWeerth, An effective lift-off method for patterning high-density gold interconnects on an elastomeric substrate, Small 6 (24) (2010) 2847–2852, https://doi.org/10.1002/smll.201001456.

[40] B. Ilic, H. Craighead, Topographical patterning of chemically sensitive biological materials using a polymer-based dry lift off, Biomed. Microdevices 2 (2000) 317–322.

[41] M. de Angelis, C. Amicucci, M. Banchelli, C. D'Andrea, A. Gori, G. Agati, C. Brunetti, P. Matteini, Rapid determination of phenolic composition in chamomile (Matricaria recutita L.) using surface-enhanced Raman spectroscopy, Food Chem. 463 (Pt 1) (2024) 141084, https://doi.org/10.1016/j.foodchem.2024.141084.

[42] C. An, S. Kim, H. Lee, B. Hwang, Facile patterning using dry film photo-resists for flexible electronics: Ag nanowire networks and carbon nanotube networks, J. Mater. Chem. C 5 (19) (2017) 4804–4809, https://doi.org/10.1039/C7TC00885F.

[43] S. Kim, J. Heo, Y. Kim, Y. Yu, C. Choi, J. Yu, Hardness of Rinse Water and Swelling Behavior of Dry Film Photo-Resist. Paper Presented at the 37th International Symposium for Testing and Failure Analysis American Society for Metals. Conference Paper Retrieved from, 2011.
[44] X. He, C. Fan, Y. Luo, T. Xu, X. Zhang, Flexible microfluidic nanoplasmonic sensors for refreshable and portable recognition of sweat biochemical fingerprint, NPJ Flexible Electronics 6 (1) (2022), https://doi.org/10.1038/s41528-022-00192-6.
[45] H. Hiramatsu, F. Osterloh, pH-controlled assembly and disassembly of electrostatically linked CdSe− SiO_2 and Au− SiO_2 nanoparticle clusters, Langmuir 19 (17) (2003) 7003–7011.
[46] Y. Huang, W. Liu, D. Wang, Z. Gong, M. Fan, Evaluation of the intrinsic pH sensing performance of surface-enhanced Raman scattering pH probes, Microchem. J. 154 (2020), https://doi.org/10.1016/j.microc.2019.104565.
[47] H. Ha, N. Qaiser, T. Yun, J. Cheong, S. Lim, B. Hwang, Sensing mechanism and application of mechanical strain sensor: a mini-review, Facta Universitatis, Series Mech Eng 21 (2023) 751–772, https://doi.org/10.22190/FUME230925043H.
[48] K. Haeji, Q. Nadeem, H. Byungil, Electro-mechanical response of stretchable pdms composites with a hybrid filler system, Facta Universitatis, Series Mech Eng 21 (2023) 51–61, https://doi.org/10.22190/FUME221205002K.
[49] C. Choi, N. Qaiser, B. Hwang, Mechanically pressed polymer-matrix composites with 3d structured filler networks for electromagnetic interference shielding application, Facta Universitatis, Series. Mech Eng. (2024), https://doi.org/10.22190/FUME240601038C.
[50] H. Ha, S. Müller, R.-P. Baumann, B. Hwang, Peakforce quantitative nanomechanical mapping for surface energy characterization on the nanoscale: A mini-review, Facta Universitatis, Series Mech Eng 22 (2024) 1–12, https://doi.org/10.22190/FUME221126001H.
[51] Y. Han, P. Matteini, B. Hwang, Fabrication method of colloidal dispersions and substrates for detection of pesticide, veterinary drug, and biomolecule using surfaced-enhanced Raman spectroscopy: a review, Applied Spectroscopy Reviews (2024) 1–22, https://doi.org/10.1080/05704928.2024.2367450.